PHILOSOPHICAL TRANSACTIONS OF THE ROYAL SOCIETY A MATHEMATICAL, PHYSICAL & ENGINEERING SCIENCES

# The liquid–vapour phase transition in fluid metals

Friedrich Hensel

*Phil. Trans. R. Soc. Lond. A* 1998 **356**, 97-117
doi: 10.1098/rsta.1998.0152

The Royal Society

# The liquid–vapour phase transition in fluid metals

By Friedrich Hensel

*Institute of Physical Chemistry, Nuclear Chemistry and Macromolecular Chemistry, University of Marburg, Hans-Meerwein-Strasse, D-35032 Marburg, Germany*

Fluid metals are typical examples of materials whose electronic structures depend strongly on the thermodynamic state of the system. The most striking manifestation of this state dependence is the metal–non-metal transition which occurs when the dense liquid evaporates to the dilute vapour or when the fluid is expanded by heating to its liquid–vapour critical point.

The main emphasis of the paper is on the intimate interplay between the changes in interparticle forces and the changes in the electronic structure associated with the metal–non-metal transition. The most significant experiments relevant to this question are those on the liquid–vapour coexistence curves, the static- and dynamic-structure factors $S(Q)$ and $S(Q,\omega)$, the electrical properties and interfacial features in the liquid vapour–critical region. For example, reflectivity experiments on mercury against sapphire reveal clearly the existence of a prewetting transition. The transition line starts at the wetting transition temperature $T_{\mathrm{w}}$. $T_{\mathrm{w}}$ lies in the metal–non-metal transition region.

**Keywords: expanded fluid metals; liquid–vapour transition; critical phenomena; wetting transition; minimum metallic conductivity; electron correlation**

## 1. Introduction

An important open problem in the statistical mechanics of fluids is an understanding of the interrelation of the metal–non-metal transition and the liquid–vapour phase transition in metallic systems. It is now 50 years since Landau & Zeldovitch (1943) first called attention to this question, specifically in relation to liquid mercury. Yet today we are still in serious need of improvements in the predictions and calculations of the volumetric and thermodynamic behaviour of metals over both vapour and liquid regions. One of the difficulties in dealing with these systems is that the electronic and molecular structures of the two phases, liquid and vapour, in equilibrium may be vastly different. For example, liquid mercury and caesium near their normal melting points are considered as normal liquid metals with properties typical of the condensed state. The small changes of basic properties such as the electrical conductivity or magnetic susceptibility on melting (Shimoji 1977) show that the electronic structure of the liquid is quite similar to that of the crystalline solid. This behaviour is usually explained, first, by the fact that the short-range atomic correlations and the atomic volume in the liquid near the normal melting point are closely similar to those of the crystal. Second, for most metals the ionic charges are so well screened by the high density of conduction electrons that the absence of long-range order in the ionic potentials of the liquid is relatively unimportant and both liquid and solid

can be reasonably well described by the nearly free-electron (NFE) approximation (Shimoji 1977).

In contrast to melting, however, there are substantial changes in the nature of the bonding of metals upon evaporation, at which point both the volume and the electronic structure change dramatically on passing from one phase to the other. At sufficiently low densities, in the vapour phase, the valence electrons occupy spatially localized atomic or molecular orbitals. In this state many caesium atoms form chemically bound dimers with a dissociation energy of 0.45 eV, whereas in the vapour phase of mercury, chemically bonded dimers do not form because the ground state of the mercury atom arises from a closed shell electronic configuration which by itself cannot form an appreciable bond owing to the inert character of the $6s^2$ shell. The interaction potential between two mercury atoms is thus generally regarded as acting between highly polarizable closed-shell systems involving very little electronic density migration from the partners, in a similar way to noble gas atoms. In this sense, mercury vapour has been denoted 'pseudo-helium' (Pyykkö 1978), while the vapour of the alkali metal caesium resembles hydrogen (Ashcroft 1990).

Whilst the two limiting cases of the dense metallic liquid and the low density insulating vapour phase are reasonably well understood, our knowledge of the connection between these two limits through the liquid–vapour critical and supercritical regions of the phase diagram lags far behind. Nearer to the critical point, the liquid density is much less and the vapour density much greater. At what density does the vapour become metallic or the liquid non-metallic? It is the variation of the interaction in the neighbourhood of the metal–non-metal transition that is difficult to deal with theoretically and which has important consequences for the liquid–vapour critical-point phase transition.

The problem that throughout the fluid range of a metal the electronic structure can change significantly with density and temperature has stimulated extensive experimental and theoretical effort and the general subject has repeatedly been reviewed in the literature (Freyland & Hensel 1985; Endo 1982; Alekseev & Jakubov 1983; Hensel 1990; Cusack 1978; Yonezawa & Ogawa 1982; Hensel & Uchtman 1989; Hensel & Hohl 1994; Hensel 1995). A comprehensive review of the subject is therefore unnecessary and I shall refrain from any attempt to cover the entire field. Instead I have selected for attention recent experimental results in the liquid–vapour critical region of metals which show that the existence of the metal–non-metal transition noticeably influences the thermodynamic, structural, interfacial and dynamic features of these metals.

## 2. Divalent metals

Mercury is the only divalent metal that has proven accessible to study in the region of its liquid–vapour critical point which is located at $T_c = 1478\ ^\circ\mathrm{C}$, $p_c = 1673$ bar and $\rho_c = 5.8\ \mathrm{g\ cm^{-3}}$. It has the lowest known critical temperature of any fluid metal. This fact is important in view of the difficulties associated with accurate measurements of physical properties at high temperatures and pressures. It is also considerably less corrosive than many metals, including the alkali metals discussed in § 3. These relatively favourable conditions have permitted very accurate measurements of its electrical, magnetic, optical, structural, interfacial and thermophysical properties with optimal temperature control to determine the asymptotic behaviour of these properties as the liquid–vapour coexistence curve, including the critical point, is approached.

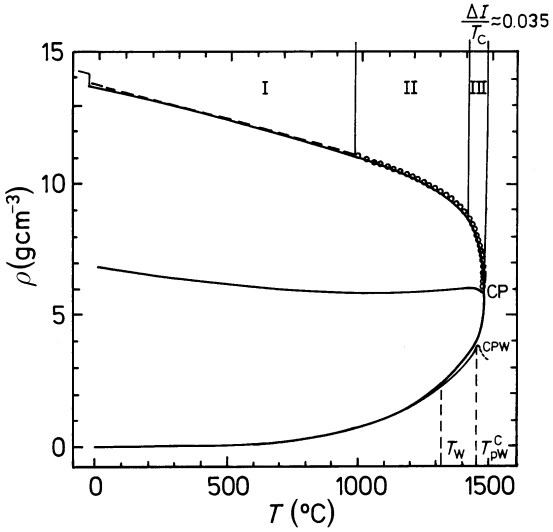


Figure 1. The bulk coexistence curve of mercury, along with the mean of the densities $\rho_L$ and $\rho_v$, the so-called diameter. The prewetting line terminates at high temperatures at the prewetting critical temperature $T_{pw}^c$ and at low temperatures at the wetting temperature $T_w$. The dashed extension of the prewetting line is a line of maximum two-dimensional compressibility in the prewetting supercritical one-phase region.

### (*a*) *Liquid–vapour and metal–non-metal transition*

The most significant experiments for the exploration of the relationship between the liquid–vapour and metal–non-metal transitions in fluid mercury are measurements of these properties over the whole liquid–vapour region along the coexistence curve. The latter is shown in figure 1, along with the mean of the densities $\rho_L$ and $\rho_v$ of coexisting liquid and vapour phases, the so-called diameter. Three ranges, denoted I, II and III, can be distinguished. In region I between the melting temperature $T_m = 38\,^\circ\mathrm{C}$ and $T = 980\,^\circ\mathrm{C}$, the density of the coexisting liquid decreases from $\rho_m = 13.65\,\mathrm{g\,cm^{-3}}$ to $11\,\mathrm{g\,cm^{-3}}$. The conductivity, $\sigma$, at $\rho_m$ is about $10^4\,\Omega^{-1}\,\mathrm{cm^{-1}}$ and the nearly free-electron (NFE) theory gives an electron mean free path of about 7 Å which exceeds only slightly the mean interatomic distance. Application of the NFE model leads to the conclusion that $\sigma$ can be satisfactorily explained if the effect of the atomic d-states is included in the pseudo-potential (Evans 1970). Mercury is thus essentially a NFE metal at $\rho_m$, despite the comparatively small mean free path.

There is, however, evidence from photoelectron spectroscopy experiments (Oelhafen *et al.* 1988) for a slight minimum in the density of states at the Fermi energy, i.e. a weak pseudo-gap. As is well known, a low-density divalent metal such as mercury is predicted by the Bloch–Wilson band model (Wilson 1931), to undergo a metal–semiconductor transition when the s- (valence) and p- (conduction) bands no longer overlap. In a crystal, a real gap appears and widens further as the density decreases. Mott (1966) has proposed that the main features of the crystalline model survive in the liquid state with the band edges smeared out by disorder. Thus, the density of states, $N(E)$, is expected to tail into the gap owing to the loss of longe-range order. The tails eventually overlap in the region of the Fermi energy $E_F$. The pseudo-gap depends strongly on density. When the magnitude of $N(E)$ in the pseudo-gap decreases at sufficiently low density to a negligibly small value, the

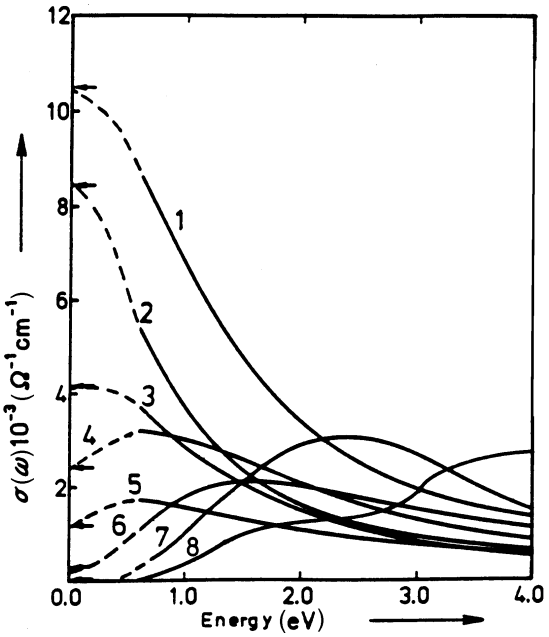


Figure 2. Optical conductivity $\sigma(\omega)$ of liquid mercury at conditions near the liquid–vapour coexistence; the corresponding densities $\rho$ and temperatures $T$ are given as follows: 1, 13.65 g cm$^{-3}$ at 25 °C; 2, 12.80 g cm$^{-3}$ at 400 °C; 3, 11.80 g cm$^{-3}$ at 810 °C; 4, 11.00 g cm$^{-3}$ at 1090 °C; 5, 10.10 g cm$^{-3}$ at 1250 °C; 6, 9.00 g cm$^{-3}$ at 1390 °C; 7, 8.00 g cm$^{-3}$ at 1450 °C; 8, 7.00 g cm$^{-3}$ at 1450 °C.

properties of mercury must become compatible with the opening-up of an energy gap.

The existence of a weak pseudo-gap in the density range near $\rho_{\mathrm{m}}$ does apparently not affect the conductivity. The NFE character in this density range is, in fact, further confirmed by the observation that the low-frequency optical conductivity $\sigma(\omega)$ shows Drude-like behaviour (see Hefner *et al.* 1980; Ikezi *et al.* 1978; and figure 2) and the Hall coefficient $R_{\mathrm{H}}$ (Even & Jortner 1972) retains the free electron value $R_{\mathrm{H}} = 1/n_{\mathrm{e}}e$ with $n_{\mathrm{e}}$ given by the total number of valence electrons, i.e. two per mercury atom. The Hall coefficient begins to deviate slightly from the free electron value for densities between 12 and 11 g cm$^{-3}$ where also changes in the shapes of the $\sigma(\omega)$ curves indicate a gradual diminution of metallic properties.

Whereas the deviation of $R_{\mathrm{H}}$ and $\sigma$ from NFE behaviour is relatively small in the density region $11 \leqslant \rho \leqslant 13.65$ g cm$^{-3}$, i.e. in region I, further expansion of mercury to a density of about 9 g cm$^{-3}$ in region II reduces $\sigma$ to a value of about 450 $\Omega^{-1}$ cm$^{-1}$ and $R_{\mathrm{H}}$ increases by about a factor of three above the free-electron value. It is often assumed that a liquid conductor at high temperatures has undergone a change from metallic to non-metallic behaviour if its $\sigma$-value falls below a few hundred $\Omega^{-1}$ cm$^{-1}$, the range of the 'minimum metallic conductivity' (Mott & Davies 1979; Mott 1974). But the magnitude of $\sigma$ alone is not sufficient evidence and the fact that for densities smaller than 9 g cm$^{-3}$ the shape of the $\sigma(\omega)$ curves is that of a substance with a real energy gap (Hefner *et al.* 1980; Ikezi *et al.* 1978) is a much more convincing sign that a range of energy around the Fermi energy exists that is so thinly populated with states that the contribution to the optical properties is negligible small. This view is strongly supported by the sharp drop of the Knight shift (Warren & Hensel 1982) for densities

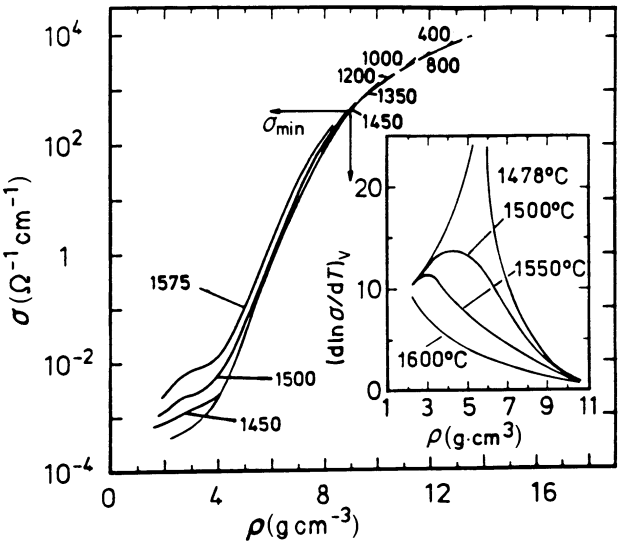


Figure 3. Electrical conductivity, $\sigma$, of fluid mercury at constant subcritical and supercritical temperatures as a function of density, $\rho$. The temperatures are in degrees Celsius. The inset shows the constant-volume temperature coefficient $[\partial(\ln\sigma)/\partial T]_\mathrm{v}$ at constant temperatures as a function of density. The arrows denote to density (and the DC conductivity) at which a gap opens in liquid mercury (see text).

smaller than 9 g cm$^{-3}$ and by calculations of the total and partial densities of states at densities along the coexistence curve employing *ab initio* density-functional molecular dynamics techniques (Kresse & Hafner 1997). The central results of these calculations is that in fluid mercury decreasing density leads to a narrowing of the s- and p-bands and finally to the metal–non-metal transition of the band-crossing type.

In principle, one might hope to determine the energy gap experimentally by identifying it with the activation energy of the conductivity which successfully describes the temperature dependence of the conductivity in crystalline and amorphous solid semiconductors. However, in high-temperature liquids such as mercury not too far from its critical point, strong fluctuations in local density become important. Hence, there is ample reason to distrust the application of solid state concepts. The importance of density fluctuations in fluid mercury for densities, $4\,\mathrm{g\,cm}^{-3} < \rho < 8\,\mathrm{g\,cm}^{-3}$, in the temperature region around $T_\mathrm{c}$, i.e. in region III, is evident from a glance at figure 3 which shows the DC conductivity $\sigma$ and the constant volume temperature coefficient $[\partial(\ln\sigma)\partial T]_\mathrm{v}$ (see inset of figure 3) plotted versus the density for various temperatures. The strong temperature dependence of $[\partial(\ln\sigma)\partial T]_\mathrm{v}$ around the critical density of 5.8 g cm$^{-3}$ is an obvious indication that effects connected with the critical point fluctuations begin to play a role. This is consistent with the observation (Götzlaff 1988) that the isothermal compressibility and the isobaric expansivity begin to rise quite rapidly as the density falls below 8 g cm$^{-3}$. The analysis of any property has to take into account the effect of these fluctuations close to $T_\mathrm{c}$. Still, there is clear-cut experimental evidence from optical absorption (Uchtmann & Hensel 1975; Yao 1994) and reflectivity measurements (Uchtmann *et al.* 1988) that the gap increases rapidly with decreasing density for $\rho$ smaller 9 g cm$^{-3}$. Ultimately, in the limit of very low density, the gap approaches the ionization potential of 10.4 eV.

There is no discontinuity in the density dependence of $\sigma$ when the gap opens at 9 g cm$^{-3}$ because the very high temperature smears out the transition range by

considerable thermal excitation of electrons. The only visible effect of the transition on the electrical conductivity in figure 3 is that $\sigma$ falls more rapidly as the density decreases below $9\,\mathrm{g\,cm^{-3}}$. It was suggested by Mott (1966) that the turnover at about $200\,\Omega^{-1}\,\mathrm{cm}^{-1}$ (figure 3) represents the minimum metallic conductivity.

### (*b*) *Interatomic interaction and structure*

It is evident from the foregoing that throughout the fluid range of mercury the electronic structure changes significantly. This implies that also the nature of the interparticle interaction must change strongly with the thermodynamic state. This strong state dependence of the interatomic interaction, in particular in the transition range where metallic properties evolve continuously into those characteristics of non-metals, has been a primary motivation for energy-dispersive X-ray diffraction measurements of the static structure factors $S(Q)$ of fluid mercury over the whole liquid–vapour density range (Tamura & Hosokawa 1994). Typical results are represented in figure 4 in the form of Fourier transforms of $S(Q)$, that is the pair correlation functions $g(R)$, at different temperatures and densities. The liquid structure just above the melting point (e.g. at 20 °C and $13.55\,\mathrm{g\,cm^{-3}}$) can be regarded as built up of single screened ions with interactions described by effective density-dependent spherically symmetric pairwise potentials. This view is prompted by the experimental observation that relatively little change in the local atomic arrangement occurs during melting. For mercury, the molar volume increases by only about 3.6%, and the average near -neighbour distance, given by the position of the first peak of the radical distribution function $g(R)$ in figure 4, is almost identical with the average near-neighbour distance $R_{\mathrm{sol}}$ in the crystalline structure close to melting. Thus the essential monatomic character of the crystal seems to be preserved through the melting transition. The latter is supported by calculations of the atomic structure of liquid mercury near the melting point employing *ab initio* density-functional molecular dynamic techniques (Götzlaff 1988) as well as by classical molecular-dynamics simulations based on effective interatomic forces derived from perturbation theory using pseudo-potentials which take into account the effect of the d-electrons (Jank & Hafner 1990).

Monatomic character dominates also in the coexisting vapour phase. Chemically bound mercury dimers do not form because the ground state of the mercury atom is a closed shell $6s^2$ electronic configuration. Nevertheless, there is still a weak attraction between mercury atoms, similarly to that between rare-gas atoms. Indeed, at $\rho = 1.89\,\mathrm{g\,cm^{-3}}$ and $T = 1350$ °C (figure 4), the first peak in $g(R)$ falls at the equilibrium distance $R_{\mathrm{Hg_2}} = 3.63$ Å of the mercury dimer potential evaluated from spectroscopic data of the isolated $Hg_2$ species formed in a molecular beam (Koperski *et al.* 1994). This value is much greater than the next-neighbour distance in the dense coexisting liquid, indicating that the effective interatomic interaction does indeed change with density.

It is immediately evident from a glance at figures 4 and 5 that the structural implications of this density dependence of the effective interaction are particularly evident in the range where the gradual diminution of metallic properties in expanded fluid mercury occurs. With decreasing density or increasing temperature a number of changes in $g(R)$ are noteworthy. First, the intensities of the main peak of $g(R)$ are strongly reduced and broadened. The pair correlation function $g(R)$ is related to the radial distribution function $n(R) = 4\pi R^2 n g(R)$ which determines the number of $n(R)\,\mathrm{d}R$ of neighbouring atoms in a spherical shell of radius $R$ and thickness $\mathrm{d}R$

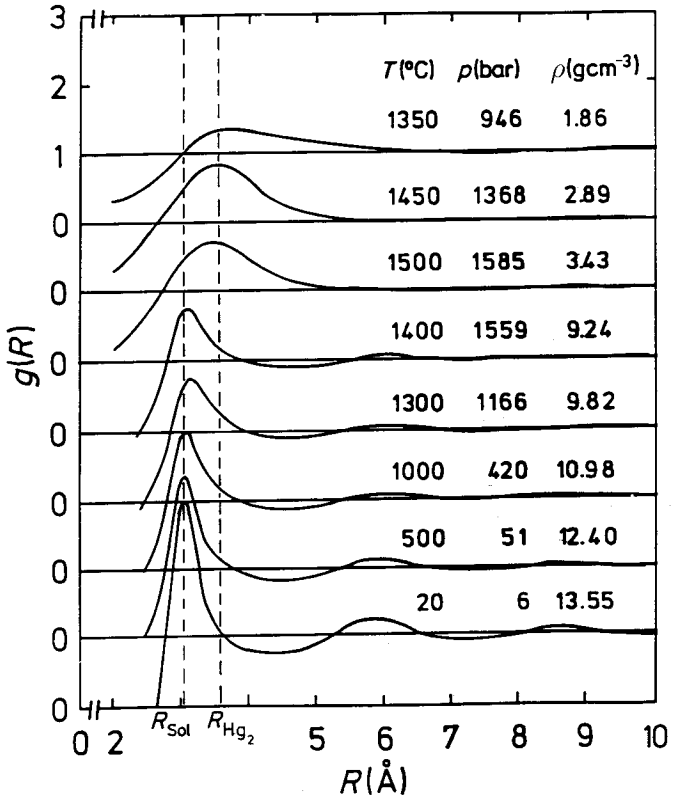


Figure 4. Pair correlation function of mercury at different temperatures and densities (Tamura & Hosokawa 1994).

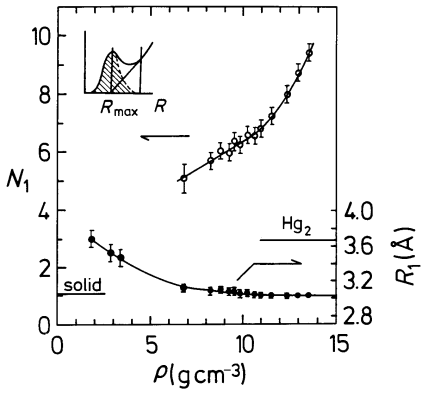


Figure 5. Average number, $N_1$, of nearest neighbours for expanded mercury together with the average next neighbour distance, $R_1$, of mercury as a function of density, $\rho$ (Tamura & Hosokawa 1994).

centred on a particular atom of interest. The average coordination number $N_1$ is determined by the area under the first peak in $n(R)$, whereas the average nearest-neighbour distance, $R_1$, is given by the position of the first peak of $g(R)$. An analysis of data such as those displayed in figure 4 for mercury is shown in figure 5 in form of $N_1$ and $R_1$ as a function of density.

The most significant aspect of the structural data in figure 5 is that, within the range of NFE behaviour between 13, 55 and 12 g cm$^{-3}$, thermal expansion proceeds by a structural evolution in which the average coordination number decreases roughly in proportion to the density while the average near-neighbour distance remains nearly constant. Such changes in shape and position of the pair correlation function are usually observed for fluids for which the nature of the effective pair interaction does not markedly change with liquid density (Winter *et al.* 1987; Mikolaj & Pings 1967). However, it is immediately evident from a glance at figure 5 that this structural trend changes in a noteworthy way for densities smaller than 12 g cm$^{-3}$ that is where the Hall coefficient, $R_{\mathrm{H}}$, and the shape of $\sigma(\omega)$ indicate that the diminution of metallic properties sets in. The decrease in the average coordination number becomes distinctly smaller whereas the average near-neighbour distance gradually increases. This observation clearly demonstrates the interplay between changes in the electronic structure and the thermodynamic and structural properties of expanded liquid mercury.

Finally, in the vapour phase, $R_1$ approaches the equilibrium distance, $R_{\mathrm{Hg}_2}$ of the weakly attractive potential of the mercury dimer. This species has been the subject of numerous experimental studies from which different pair potential models for its ground state have been derived. It was concluded from such investigations that it is a weakly bound van der Waals molecule. However, recent quantitative studies of the depolarized interaction-induced light scattering (DILS) spectra of mercury vapour as a function of density and temperature (Barocchi *et al.* 1995) indicate that mercury behaves differently from inert gases. The DILS data have been used to derive the form of the interaction-induced pair polarizability anisotropy. The result of this analysis is that mercury pairs formed during collisions develop an incremental polarizability in addition to the dipole-induced dipole (DID) contribution. This effect is particularly important at short- and intermediate-range distances and has to be ascribed to other mechanisms of electron cloud distortion, such as overlap, 6s→6p interatomic excitation, and electron correlation effects. The development of a large positive intermediate-range pair polarizability anisotropy reveals the breakdown of the simple classical DID approximation and the onset of specific interactions in the electronic properties. This makes mercury pair interaction properties not completely van der Waals in nature and therefore quite different from noble gases. This view is consistent with an *ab initio* study of the individual interaction energy components in the ground state of the mercury dimer (Kunz *et al.* 1996). These calculations show that induction effects play an important role in the stabilization of $Hg_2$, unlike the situation commonly encountered for the inert gas dimers. There the assumption of unperturbed monomer electron densities is normally justified. Since the short-range induction effects lead to a significant energy lowering, the mercury dimer may be regarded as an intermediate case between a weakly bound van der Waals molecule and a chemically bonded species. Induction contributions to the bonding energy are a first indication that mercury clusters undergo a transition from weak to covalent and finally to metallic bonding (Rademann *et al.* 1987).

### (*c*) *Critical phenomena*

It is evident from the foregoing that a fundamental distinction between fluid metals and insulating fluids such as inert gases lies in the character of the interparticle interaction. An inert gas atom retains its identity in the condensed phase. In contrast, the electronic structures of the two coexisting phases, liquid and vapour, of

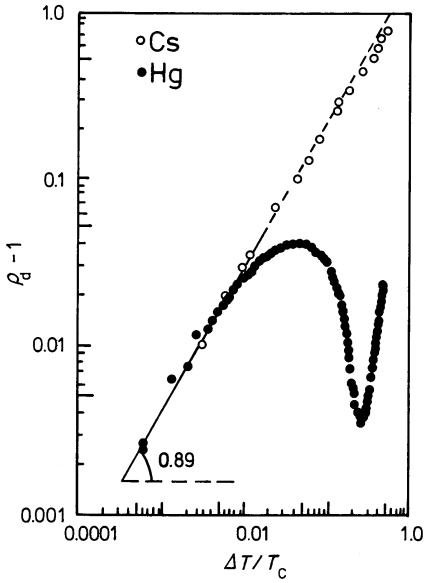


Figure 6. Power-law analysis of the diameters of mercury and caesium.

fluid metals are very different. Far below the critical temperature, the vapour phase is non-metallic with weak interatomic or intermolecular interactions. In contrast, the coexisting liquid is highly conducting and the interaction is dominated by screened Coulomb potentials. However, the presence of strong state-dependent interactions in metals does not imply that the critical behaviour of the thermodynamic properties cannot be described with the same exponents as that of molecular fluids. The speculation that critical points of metals could belong to a different universality class than molecular fluids, which was mainly based on the assumption that the Hamiltonian of metallic systems consists of a sum of long-range Coulomb interactions has been clearly ruled out by accurate measurements of the shapes of the coexistence curves of mercury (Götzlaff 1988), cesium and rubidium (Jüngst *et al.* 1985). There is no doubt that they display the same critical exponents as molecular fluids, i.e. values close to those found for the three-dimensional Ising-model.

The implications of the state dependence of the interatomic interactions for the liquid–vapour phase equilibrium of metals are mainly evident from the behaviour of the diameter $\rho_d = \rho_L + \rho_v/2\rho_c$ (see figures 1 and 6) in the transition range where metallic properties evolve continuously into those characteristic of non-metals. Indeed far from the critical point in range I of figure 1, $\rho_d$ has a positive slope as is typical of molecular fluid (Levelt Sengers *et al.* 1983) and as is also observed for the alkali metals (Jüngst *et al.* 1985). In this region the coexisting liquid is metallic ($\rho \geqslant 11\,\mathrm{g\,cm^{-3}}$) while the vapour consists of atoms interacting through weak forces. At higher temperatures, i.e. in range II, where the liquid is in the electronic transition range, $\rho_d$ slopes toward higher densities, opposite to the behaviour seen in molecular fluids and the alkali metals. Thus, one observes at a density of about $11\,\mathrm{g\,cm^{-3}}$ a clear correlation between an anomaly in the diameter slope and a change in the electronic structure demonstrating the interplay between the latter and the liquid–vapour phase behaviour.

Within the critical region of mercury (range III in figure 1), there does indeed appear the theoretically expected $(1-\alpha)$ singularity. Theory predicts that the tem-

perature derivative of the diameter $\mathrm{d}\rho_\mathrm{d}/\mathrm{d}T$, diverges at least as fast as the constant-volume specific heat $c_\mathrm{v}$. That is, as the reduced temperature, $\Delta T/T_\mathrm{c}$, goes to zero, the diameter varies as

$$\rho_\mathrm{d} = 1 + D_0 \left(\frac{\Delta T}{T_\mathrm{c}}\right)^{1-\alpha} + D_1 \left(\frac{\Delta T}{T_\mathrm{c}}\right).$$

The linear term is the usual background rectilinear diameter observed in all fluids. The term $D_0(\Delta T/T_\mathrm{c})^{1-\alpha}$, where $\alpha = 0.11$ is the same exponent as that which characterizes the power-law divergence of the specific heat along the critical isochore.

It is evident from a glance at figure 6 that the critical diameter anomalies for the alkali metals and mercury are characterized by exponents $(1-\alpha)$. For the alkali metals the anomalies are so strong that a nearly pure power-law behaviour is seen over several decades in the reduced temperature $\Delta T/T_\mathrm{c}$. The competing variations of the electronic structure of liquid mercury with density and temperature cause a pronounced wiggle at intermediate $\Delta T/T_\mathrm{c}$ values.

Another interesting example of the intimate interplay between changes in interparticle forces and changes in the electronic structure associated with the liquid–vapour critical point phase transition in mercury is provided by recent experimental work (Hensel 1995; Hensel & Yao 1994; Yao & Hensel 1996; Kozhevnikov *et al.* 1997) on the wetting behaviour of mercury films on rigid solids. Whilst most pure liquid metals wet completely a perfectly clean solid metal surface, it has been known for a long time, that the low surface free energy of most non-metallic solids precludes their being wetted by 'inert' (non-reactive) liquid metals. Indeed, the closest example in common experience of a non-wetting substance is liquid mercury on glass or on oxide or sulfide layers on metals, even if—as is usually the case—the oxide layer is extremely thin. The liquid (L) forms a drop on the solid substrate (S) characterized by the angle of contact, $\vartheta$, which is obtained using Young's equation:

$$\cos\vartheta = (\gamma_\mathrm{SV} - \gamma_\mathrm{SL})/\gamma_\mathrm{LV},$$

where the subscripts SV and SL refer to the solid interfacing with, respectively, the saturated vapour and coexisting liquid, $\gamma_\mathrm{LV}$ is the interfacial tension between the liquid and the vapour phases. For mercury on glass, quartz and sapphire, $\vartheta$ is at room temperature far beyond 90 °C. Then the liquid is said to partially wet the substrate. For such a situation it has been argued (Cahn 1977; Ebner & Saam 1977) that there may exist a particular temperature, $T_\mathrm{w}$, at which one switches from partial wetting to complete wetting with a strictly vanishing contact angle, $\vartheta$. $T_\mathrm{w}$ is the wetting transition temperature. For $T \geqslant T_\mathrm{w}$, a macroscopically thick film wets the solid substrate at coexistence. The wetting transition can be either continuous or first order. If the transition is first order, with a continuous jump in the film thickness on the coexistence curve, thermodynamics requires that it is accompanied by a line of prewetting transitions (Cahn 1977; Ebner & Saam 1977). These are transitions from a thin to a thick liquid layer, induced, for example, by increasing $p$, the pressure of the vapour, towards its value on bulk saturation, $p_\mathrm{sat}(T)$, at a fixed temperature $T$, above the wetting temperature, $T_\mathrm{w}$. The line of first-order prewetting transitions extends smoothly from the point of the first order wetting transition ($T_\mathrm{w}$, $p_\mathrm{sat}$) into the region of unsaturated films with $p < p_\mathrm{sat}$. It is expected to terminate at a prewetting critical point ($T^\mathrm{c}_\mathrm{pw}$, $p^\mathrm{c}_\mathrm{pw}$), where the distinction between thin and thick films disappears.

As mentioned above, an obvious candidate for a prewetting transition is mercury

on a non-metallic substrate. While strictly speaking, the wetting transition from partial to complete wetting is not necessarily a critical phenomenon, it is expected (Cahn 1977) to show up when liquid mercury is heated to the region of its liquid–vapour critical point.

This prewetting transition has been detected in mercury (Hensel & Yao 1994; Yao & Hensel 1996) by reflecting light from a vertical sapphire–mercury interface. To locate the prewetting line, reflectivity measurements were performed at constant temperature $T$ by increasing $p$, the pressure of the vapour, towards its value at bulk saturation $p_{\mathrm{sat}}$ or alternatively at constant $p$ by increasing $T$ towards $T_{\mathrm{sat}}$. Quantitative analysis of the different isotherms and isobars in combination with the known equation-of-state data for fluid mercury allows one to construct the prewetting phase diagram in the density $\rho$–temperature $T$ plane as displayed in figure 1. The prewetting line meets the bulk liquid–vapour coexistence curve tangentially at the prewetting temperature $T_{\mathrm{w}} = 1310\,^{\circ}\mathrm{C}$, and terminates at the prewetting critical temperature $T_{\mathrm{pw}}^{\mathrm{c}} = 1468\,^{\circ}\mathrm{C}$ and prewetting critical pressure $p_{\mathrm{pw}}^{\mathrm{c}} = 1586$ bar lying close to the bulk critical point. $T_{\mathrm{pw}}^{\mathrm{c}}$ divides the curve in figure 1 into two parts: for $T_{\mathrm{w}} < T < T_{\mathrm{pw}}^{\mathrm{c}}$ the curve defines the prewetting thick–thin coexistence region; while for $T > T_{\mathrm{pw}}^{\mathrm{c}}$ the curve marks the location of the dashed extension of the prewetting line which displays the line of maxima in the two-dimensional compressibility of the prewetting supercritical one-phase region.

An interesting observation is that $T_{\mathrm{w}}$ lies in the range where the gradual diminution of metallic properties occurs in liquid mercury at coexistence. The frequency dependence of $\sigma(\omega)$ (figure 2) clearly shows that for temperatures higher than 1300 °C a range of energy (a pseudo-gap) exists that is so thinly populated with states that the contribution to $\sigma(\omega)$ is small. It can be expected that the opening of an effective gap strongly affects the wetting behaviour of mercury.

As is well known, the wetting of solids by liquids is strongly influenced by the interaction between the solid–liquid interface and the liquid–vapour interface. The original Hamaker–de Boer (Hamaker 1937; de Boer 1936) theory uses a summation of the van der Waals pair interactions between the molecules of the vapour, liquid and the solid substrate. This procedure may be an acceptable approach for a collection of poorly polarizable weakly interacting atoms or molecules. Long-range dispersion forces, however, exist and are important also in metals and semiconductors as well as in insulators, but they are certainly no longer given by the simple Hamaker–de Boer summation approach. For metals, collective effects are important and the well-known field-theoretical approach (Dzayloshinsky *et al.* 1961), which is generally valid, provides a better framework for the treatment of dispersion forces. According to this theory, there exists a van der Waals force between the polarizable media due to the fluctuations of the electromagnetic field and the discontinuity of the dielectric function across the boundaries. The general formula first derived by Dzayloshinsky *et al.* (1961) for the van der Waals chemical potential of semi-infinite solids and semi-infinite vapour, $V$, separated by a planar macroscopic slab of a liquid, $L$, of thickness $D$ is

$$\mu(D,T) = \frac{kT}{8\pi D^3}\left[\frac{1}{2}\sum_{m=1}^{\infty}\frac{\varepsilon_{\mathrm{S}}(0)-\varepsilon_{\mathrm{L}}(0)}{\varepsilon_{\mathrm{S}}(0)+\varepsilon_{\mathrm{L}}(0)}\frac{\varepsilon_{\mathrm{V}}(0)-\varepsilon_{\mathrm{L}}(0)}{\varepsilon_{\mathrm{V}}(0)+\varepsilon_{\mathrm{L}}(0)}m^{-3} + \sum_{n=1}^{\infty}\frac{\varepsilon_{\mathrm{S}}(\mathrm{i}\omega_n)-\varepsilon_{\mathrm{L}}(\mathrm{i}\omega_n)}{\varepsilon_{\mathrm{S}}(\mathrm{i}\omega_n)+\varepsilon_{\mathrm{L}}(\mathrm{i}\omega_n)}\frac{\varepsilon_{\mathrm{V}}(\mathrm{i}\omega_n)-\varepsilon_{\mathrm{L}}(\mathrm{i}\omega_n)}{\varepsilon_{\mathrm{V}}(\mathrm{i}\omega_n)+\varepsilon_{\mathrm{L}}(\mathrm{i}\omega_n)}(1+r_n)\mathrm{e}^{-r_n}\right].$$

The dielectric functions, $\varepsilon$, are evaluated at the sequence of imaginary frequencies: $(\mathrm{i}\omega_n) = \mathrm{i}(2\pi kT/\hbar)n$ and $r_n = 2D\omega_n\sqrt{\varepsilon_\mathrm{L}/c}$, where

$$\varepsilon(\mathrm{i}\omega_n) = 1 + 8\int_0^\infty \frac{\sigma(\omega)}{(\omega^2+\omega_n^2)}\,\mathrm{d}\omega$$

and $c$ is the velocity of light.

It is evident that the chemical potential can change sign and may be non-monotonic as a function of $D$. If $\varepsilon_\mathrm{L}(\mathrm{i}\omega_n) > \varepsilon_\mathrm{S}(\mathrm{i}\omega_n)$ and $\varepsilon_\mathrm{L}(\mathrm{i}\omega_n) > \varepsilon_\mathrm{v}(\mathrm{i}\omega_n)$, as is the case for metallic liquid mercury and insulating sapphire, $\mu$ is positive, corresponding to non-wetting. However, as is seen from a glance at figure 2, at temperatures close to the wetting temperature of about 1310 °C, the shape of $\sigma(\omega)$ changes to the characteristic of a substrate with a real gap, that is, the dielectric constant of the liquid $\varepsilon_\mathrm{L}(\mathrm{i}\omega_n)$, undergoes profound changes. It can be expected that such changes influence the sign and functional form of $\mu(D)$ leading to wetting.

## 3. Monovalent alkali metals

The interrelation of the metal–non-metal transition and the liquid–vapour phase transition in fluid alkali metals can be seen in much the same way that one observes it in fluid mercury—by measuring the equation of state (Jüngst *et al.* 1985) simultaneously with electrical (Freyland 1981; Hensel *et al.* 1991), optical (Knuth *et al.* 1997) or magnetic (Freyland 1979; Warren *et al.* 1989) properties. However, the transitions in these two kinds of systems, are clearly distinct. Hints at the differences show up at a glance from a comparison of the shape of the coexistence curve as discussed in § 2 *c* (see figures 1, 6 and 7). On the whole the coxistence curve of mercury is much more symmetric than that of caesium. Also the electrical properties bear a quantitative difference. Taken as a group, the alkali metals exhibit very similar electrical conductivities. At the critical point, the conductivity is about $250\,\Omega^{-1}\,\mathrm{cm}^{-1}$ for each of the three alkali metals (potassium, rubidium and caesium) that have been studied experimentally in the critical region (Freyland 1981), while that of mercury is roughly two orders of magnitude lower.

Such differences between divalent mercury and monovalent alkali metals might have been expected from the simplest considerations based on the Bloch–Wilson model. Indeed, without electron–electron interaction the latter would lead to the prediction that the alkali metals are always metallic, regardless of the density. This prediction has stimulated very early experimental attempts to observe metallic conductivity in low density alkali metal vapours (Braunbeck 1935) but thanks to the work of Mott (1949, 1961) we know now that because of electron correlations, this cannot be true. In addition, there is now considerable experimental evidence (Hensel & Hohl 1994) from magnetic-susceptibilty and optical-absorption measurements that in alkali vapours the valence electrons occupy spatially localized atomic and molecular orbitals.

### (*a*) *Liquid–vapour and metal–non-metal-transitions*

The physical consequences of the substantial changes in the electronic and molecular structures upon evaporation are vividly illustrated by data such as those displayed in figures 7 and 8 which show the most accurate density, $\rho$ and DC electrical conductivity, $\sigma$, data of the coexisting liquid and vapour phases of caesium up to the

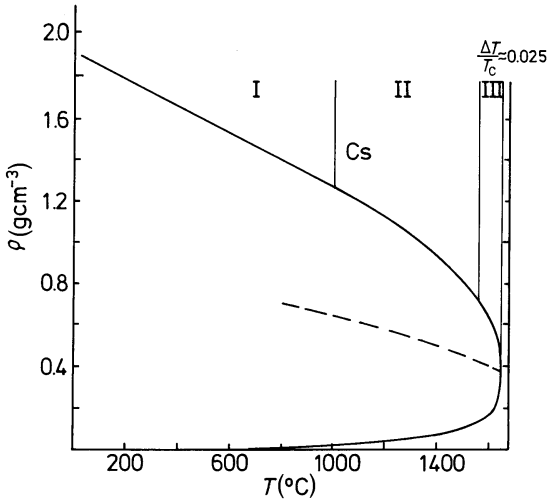


Figure 7. The bulk coexistence curve of caesium along with the mean of the densities $\rho_{\mathrm{L}}$ and $\rho_{\mathrm{v}}$, the so-called diameter.

critical point at $T_{\mathrm{c}} = 1651\,^{\circ}\mathrm{C}$ and $\rho_{\mathrm{c}} = 0.38\,\mathrm{g\,cm^{-3}}$ (Jüngst *et al.* 1985). The corresponding critical pressure is $p_{\mathrm{c}} = 92.5$ bar. As for divalent mercury, the density dependence of the conductivity may be subdivided into three domains (see figure 7). Between the melting temperature $T_{\mathrm{m}} = 30\,^{\circ}\mathrm{C}$ and $T = 1100\,^{\circ}\mathrm{C}$ the density of the liquid decreases from $\rho_{\mathrm{m}} = 1.84\,\mathrm{g\,cm^{-3}}$ to $\rho = 1.3\,\mathrm{g\,cm^{-3}}$. Throughout this range of initial expansion, the magnetic, optical and electrical properties are consistent with the NFE theory. Conductivities, calculated using this theory (Winter *et al.* 1987), match the measured values for temperatures lower than 1100 °C (figure 8). At higher temperatures, and hence lower densities, $\sigma$ is lower than that predicited by the NFE model. The gradual failure of the model at densities lower than $1.3\,\mathrm{g\,cm^{-3}}$ is probably not due to the breakdown of the NFE condition, that the electron mean free path, $\lambda$, must exceed the mean interatomic distance. Estimates of $\lambda$ from the conductivity (Winter *et al.* 1987) indicate that this condition is only reached in the density range $\rho \approx 0.8\,\mathrm{g\,cm^{-3}}$. Rather, the NFE breakdown is more likely to reflect the increased importance of electron correlations below this density. This view is based on magnetic susceptibility (Freyland 1979), NMR (Warren *et al.* 1989) and optical-reflectivity (Knuth *et al.* 1997) studies of low-density liquid caesium which have yielded evidence of strong electron–electron correlations in the form of susceptibility enhancements and antiferromagnetic spin fluctuations. The susceptibility, NMR and optical data show a relative sharp onset of a correlation enhancement of the effective electron mass at a density of $1.3\,\mathrm{g\,cm^{-3}}$. The combined analysis of the magnetic and NMR data shows that correlation enhancements of the effective mass, $m_{\mathrm{eff}} = 6m_0$, develop at a density of $0.8\,\mathrm{g\,cm^{-3}}$, i.e. at about twice the critical density.

Alternatively, the strong decrease of $\sigma$ for densities below about $1.3\,\mathrm{g\,cm^{-3}}$ can also be interpreted in terms of partial ionization due to the formation of species such as $\mathrm{Cs}^0$ atoms, $\mathrm{Cs}_2^0$ dimers and $\mathrm{Cs}_2^+$ dimers which leads to a reduction of the number of free charge carriers. This approach views the low-density liquid as the high-density limit of the compressed metal vapour. It is immediately evident from a glance at figure 8 that the formation of such species affects strongly the conductivity of the dense vapour phase of caesium. Here the measured conductivity is compared with values calculated from the thermal equilibrium fraction of ionized caesium monomers.

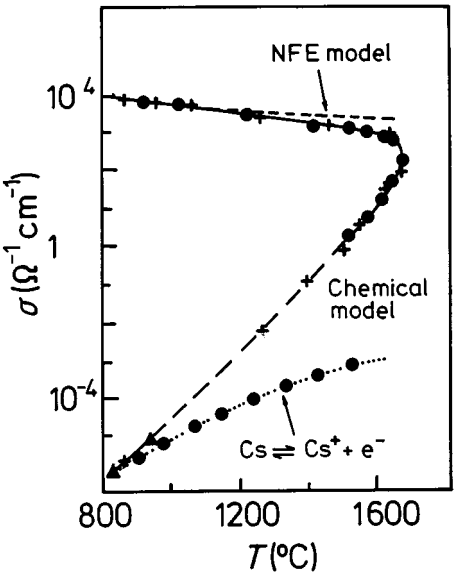


Figure 8. Experimental DC electrical conductivity, $\sigma$ (solid points), of fluid caesium as a function of temperature along the liquid–vapour coexistence line in comparison with the nearly free-electron conductivities (dashed line) and the conductivities calculated using the Saha equation (dotted line) (for details see text).

For this calculation, the vacuum ionization potential (3.89 eV) was employed in the Saha equation. Agreement between experimental and calculated values is satisfactory only at very low temperatures and densities where the overwhelmingly dominant species in the vapour is the atomic monomer. At higher vapour densities, species such as the dimer and even larger clusters appear. The ionization potentials of these clusters are much lower than that of the free atom and we should expect the degree of ionization to be much higher than given simply by the Saha equation.

The concentrations of the various species in the coexisting vapour and liquid phases have been calculated for caesium (Redmer & Warren 1993), employing a quantum statistical equation of state originally derived for partially ionized plasmas which takes into account the interaction corrections between the various species in a systematic way. An approximate self-consistent solution for the system of coupled mass action laws describes the formation of atoms ($Cs^0$) dimers ($Cs_2^0$) and molecular ions ($Cs_2^+$) out of the elementary particles, electrons $e^-$ and simple ions. The numerical results obtained for the concentrations of neutral atoms, $Cs_0$, neutral dimers, $Cs_2^0$, singly ionized dimers, $Cs_2^+$, and thermally ionized free electrons are shown as a function of density in figure 9. The results suggest that at about twice the critical density, the combined concentration of $Cs_2^0$ and $Cs_2^+$ dimers is of the order of 40%. Similar results have been obtained for fluid rubidium (Redmer & Warren 1993). The crosses in figure 8 show the conductivity calculated with the electron concentration in figure 9 (Redmer *et al.* 1992). The agreement is very good.

### (*b*) *Dynamic structure*

The problem that throughout the liquid range of an alkali metal the dynamic units can change significantly with density and temperature, i.e. that vestiges of dimers can persist in the lower-density range of the liquid, has stimulated neutron-scattering measurements of the static structure factor $S(Q)$ of caesium and rubidium

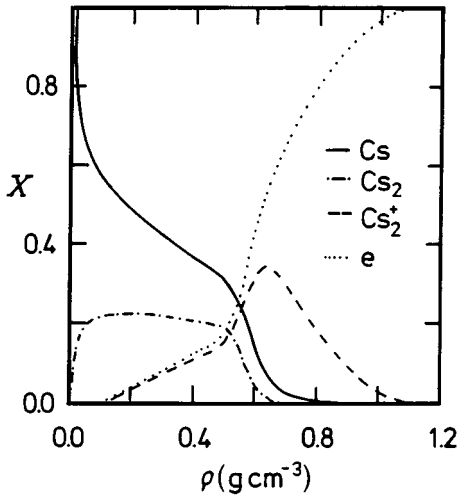


Figure 9. Relative concentrations of free conduction electrons (dotted line) and electrons localized on neutral Cs atoms (solid line), ionized $Cs_2^+$ dimers (dashed line) and neutral $Cs_2$ dimers (dashed line) as a function of density (Redmer & Warren 1993).

(Winter *et al.* 1987; Franz *et al.* 1980). The data obtained show that the dominant effect of thermal expansion of the liquid is a reduction of the average coordination number (thermal hole formation), while the average interparticle distance grows only very little. However, within standard approximations of theoretical descriptions and within experimental uncertainties, the $S(Q)$ data do not provide a clear-cut answer to the question mentioned above. The problem is that quite different views of the microscopic structure of expanded liquid alkali metals are possible to describe $S(Q)$ reasonably well.

More interesting insight into the question of whether remnants of the diatomic unit, present in the dense vapour phase of alkali metals, can survive the condensation to the liquid state can be obtained by examining recent coherent inelastic neutron-scattering spectra for liquid rubidium (Pilgrim *et al.* 1995, 1997) which extend nearly to the critical region. The critical data for Rb are: $T_c = 1744\,^\circ\mathrm{C}$, $p_c = 124.5$ bar, $\rho_c = 0.29\ \mathrm{g\ cm^{-3}}$ (Jüngst *et al.* 1985). From the early work of Copley & Rowe (1974) it is known that rubidium near its melting point at 47 °C, unlike dense Lennard–Jones (inert-gas) systems, exhibits distinct longitudinal collective excitations up to relatively high $Q$-values. The measured dispersion relation resembles very much that of longitudinal phonons in crystalline rubidium. The more recent measurements of $S(Q,\omega)$ for expanded liquid rubidium (Pilgrim *et al.* 1995, 1997) extending nearly to the critical point show that these collective excitations can be observed over a very wide temperature range up to 1400 °C.

With respect to changes in interatomic interactions associated with the metal–non-metal transition, it is most significant that high-$Q$ collective excitations are experimentally observed in liquid alkali metals, whereas they have not been detected in the insulating inert gas liquids. This distinction is reproduced well by the respective molecular dynamics calculations for these liquids. The potentials used for simulations of the inert gas liquids are the relatively short-range Lennard–Jones potentials (Sköld *et al.* 1972) whereas those used for rubidium are long-range oscillatory potentials typical for metals (Rahman 1974; Hoshino *et al.* 1992; Kahl *et al.* 1993). This suggests strongly that it is the longer range of the screened coulomb potential that causes

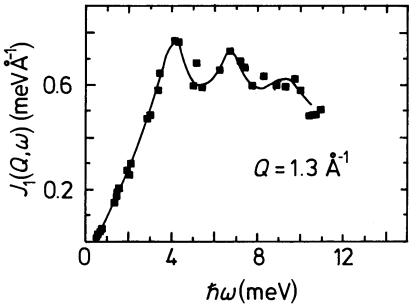


Figure 10. Experimentally determined current correlation function for liquid rubidium $J_1(Q,\omega) = (\omega^2/Q^2)S(Q,\omega)$ at $Q = 1.3\,\text{Å}^{-1}$ at $T = 1600\,^\circ\text{C}$ and $\rho = 0.61\,\text{g cm}^{-3}$. The solid line is just a guide for eye.

several ions to move coherently, even if for only a short time. As a result strongly damped, but observable collective excitations are present in the metals while they are absent in Lennard–Jones liquids.

The results of molecular dynamics calculations are in quantitative agreement with experiment for rubidium up to a temperature of 1400 °C where the density is about three times the critical density. Liquid rubidium is still basically monatomic and the screened forces typical of metallic binding still control the liquid dynamics under these conditions. This is no longer true when the temperature is increased still further and evidence of intramolecular vibrations appears. This is immediately evident from a glance at figure 10 which displays the longitudinal current correlation function $J_1(Q,\omega) = (\omega^2/Q^2)$. $S(Q,\omega)$ for $Q = 1.3\,\text{Å}^{-1}$ at 1600 °C. The liquid density at this point is $0.61\,\text{g cm}^{-3}$ about twice the critical density. Three peaks can be clearly identified as resulting from excitations at 3.2 meV with higher harmonics at 6.4 and 9.6 meV. This feature was assigned to excitation of local harmonic oscillations of pairs of rubidium atoms. These are transient dimers executing harmonic oscillations in the environment of their neighbouring atoms in the liquid.

The measured excitation energy of 3.2 meV is surprisingly close to that calculated for $Rb_2$ molecules on a simple cubic lattice (Pilgrim *et al.* 1997). These are calculations for the total energy of expanded lattices of monatomic Rb and $Rb_2$ dimers using density functional theory in the local density approximation. They were made for a system of Rb atoms in a body-centred lattice (BCC) and for diatomic molecules in a simple cubic lattice (SC). To create the diatomic solid the two atoms in the BCC unit cell were moved towards one another forming a simple cubic lattice (SC). The dimer bond length in the molecular lattice was varied to minimize the total energy. Below a density of $0.9\,\text{g cm}^{-3}$, which is about three times the critical density, $\rho_c$, the SC $Rb_2$ lattice has the lowest energy.

The vibron energy and dissociation energy were obtained by displacing the bond length from its equilibrium value $R_0$ and calculating the change in energy $E(R - R_0)$. These data were then fitted to a Morse potential. The calculations predict that the vibron and dissociation energy decrease with increasing density from their gas-phase value to zero near $0.9\,\text{g cm}^{-3}$, the corresponding number density is $6.3 \times 10^{21}\,\text{cm}^{-3}$. Such a decrease in the vibron energy with decreasing density is a well-established feature found in optical studies on solid molecular hydrogen (Mao & Hemley 1994). This decrease is believed to be associated with the transfer of electron charge towards neighbouring molecules leading to a softening of the molecular bond and the formation of a monatomic state. In the case of hydrogen the dissociation

energy is nearly an order of magnitude larger than for the alkali metals and this molecule is believed to metallize in the solid at a density of $6.6 \times 10^{23}$ (Ashcroft 1994), i.e. a density which is about 100 times that required for rubidium.

It has been often speculated (Hensel & Edwards 1996) that the differences in elemental densities at the metal–non-metal transition are related to the radius of the principal maximum in the charge density of the ns valence orbital $a^*$ which enters into the celebrated Mott criterion. The relatively small value of $a^*$ for atomic hydrogen (0.529 Å) then indicates that high densities at pressures of several megabar are required for the transition to metallic hydrogen. In contrast, the high-$a^*$ values of rubidium (2.29 Å) and caesium (2.52 Å) ensure that they are metallic at normal conditions, and that the dimerization occurs in the expanded state at a low pressure which is stabilized in the fluid at high temperatures. Obviously, at high temperatures there will be a considerable degree of dissociation and the fluid is a partially dissociated mixture of monomers and dimers (Redmer & Warren 1993; Pilgrim *et al.* 1997). Interestingly the recent experimental results for dynamically compressed fluid hydrogen (Weir *et al.* 1996) show that high temperature provides a path for metallization of fluid hydrogen at the relatively low atomic density of $3.7 \times 10^{23}$ cm$^{-3}$. At this density and temperatures of the order 3000 K a conductivity of 2000 $\Omega^{-1}$ cm$^{-1}$ is reported. This conductivity is typical of an expanded liquid alkali metal (Hensel & Edwards 1996).

## References


Alekseev, V. A. & Jakubov, I. T. 1983 *Phys. Rep.* **96**, 1.

Ashcroft, N. W. 1990 *Nuovo Cimento* **12**, 597.

Ashcroft, N. W. 1994 In *Elementary processes in dense plasmas* (ed. S. Ichimaru & S. Ogata), p. 251. Reading, MA: Addison-Wesley.

Barocchi, F., Hensel, F. & Sampoli, M. 1995 *Chem. Phys. Lett.* **232**, 445.

Braunbek, W. 1935 *Z. Phys.* **97**, 482.

Cahn, J. W. 1977 *J. Chem. Phys.* **66**, 3667.

Copley, J. R. D. & Rowe, J. M. 1974 *Phys. Rev. Lett.* **32**, 49.

Cusack, N. E. 1978 In *The metal nonmetal transition in disordered systems* (ed. L. R. Friedman & D. P. Tunstall), p. 455. Edinburgh Scottish University Summer School in Physics.

De Boer, J. H. 1936 *Trans. Faraday Soc.* **32**, 21.

Dzayloshinsky, I. E., Lifshitz, E. M. & Pitaevskii, I. P. 1961 *Adv. Phys.* **10**, 165.

Ebner, C. & Saam, W. F. 1977 *Phys. Rev. Lett.* **38**, 1486.

Endo, H. 1982 *Suppl. Prog. Theor. Phys.* **72**, 100.

Evans, R. 1970 *J. Phys.* C **2**, 137.

Even, U. & Jortner, J. 1972 *Phys. Rev. Lett.* **28**, 31.

Franz, G., Freyland, W., Gläser, W., Hensel, F. & Schneider, E. 1980 Structure of expanded liquid rubidium by neutron diffraction. In *Proc. 4th Int. Conf. of Liquid and Amorphous Metals. J. Phys. Colloq.* **C8 41**, 194–198.

Freyland, W. 1979 *Phys. Rev.* B **20**, 5104.

Freyland, W. 1981 *Comments Solid State Phys.* **10**, 1.

Freyland, W. & Hensel, F. 1985 In *The metallic and the nonmetallic states of matter* (ed. P. P. Edwards & C. N. R. Rao), p. 93. London: Taylor & Francis.

Götzlaff, W. 1988 Doctoral thesis, University of Marburg.

Hamaker, H. C. 1937 *Physica* **4**, 1058.

Hefner, W., Schmutzler, R. W. & Hensel, F. 1980 *J. Phys. Paris* **41**, C8–62.

Hensel, F. 1990 *J. Phys. Condens. Matter* **2**, SA33.

Hensel, F. 1995 *Adv. Phys.* **44**, 3.

Hensel, F. & Edwards, P. P. 1996 *Chem. Eur. J.* **2**, 1201.

Hensel, F. & Hohl, G. F. 1994 *Rev. High Pressure Sci. Technol.* **3**, 163.

Hensel, F. & Uchtmann, H. 1989 *A. Rev. Phys. Chem.* **40**, 61.

Hensel, F. & Yao, M. 1994 In *Elementary processes in dense plasmas* (ed. S. Ichimaru & S. Ogata), p. 295. Reading, MA: Addison-Wesley.

Hensel, F., Stolz, M., Hohl, G., Winter, R. & Götzlaff, W. 1991 *J. Phys. Colloq.* **C5** suppl. **1**, 191–205.

Hoshino, K., Ugawa, H. & Watabe, J. 1992 *Phys. Soc. Japan* **61**, 2182.

Ikezi, H., Schwarzenegger, K., Simons, A. L., Passner, A. L. & McCall, S. L. 1978 *Phys. Rev.* B **18**, 2494.

Jank, W. & Hafner, J. 1990 *Phys. Rev.* B **42**, 6926.

Jüngst, S., Knuth, B. & Hensel, F. 1985 *Phys. Rev. Lett.* **55**, 2160.

Kahl, G., Kambayashi, S. & Nowotny, G. 1993 *J. Non-Cryst. Solids* **15**, 156.

Knuth, B., Hensel, F. & Warren Jr, W. W. 1997 *J.Phys. Condens. Matter* **9**, 2693.

Koperski, J., Atkinson, J. B. & Krause, L. 1994 *Chem. Phys. Lett.* **219**, 161.

Kozhevnikov, V. F., Arnold, D. I., Naurzakov, S. P. & Fisher, M. E. 1997 *Phys. Rev. Lett.* **78**, 1735.

Kresse, G. & Hafner, J. 1997 *Phys. Rev.* B **55**, 7539.

Kunz, C. F., Hättig, C. & Hess, B. A. 1996 *Mol. Phys.* **89**, 139.

Landau, L. & Zeldovitch, G. 1943 *Acta Phys. Chem. USSR* **18**, 1940.

Levelt Sengers, J. M. H., Morrison, G. & Chang, R. 1983 *Fluid Phase Equilibria* **14**, 19.

Mao, H. K. & Hemly, R. J. 1994 *Rev. Mod. Phys.* **66**, 671.

Mikolaj, P. G. & Pings, C. 1967 *J. Chem. Phys.* **46**, 1401.

Mott, N. F. 1949 *Proc. Phys. Soc. Lond.* **62**, 419.

Mott, N. F. 1961 *Philos. Mag.* **6**, 287.

Mott, N. F. 1966 *Phil. Mag.* **13**, 989.

Mott, N. F. 1974 *Metal–insulator transitions* London: Taylor & Francis (and references therein).

Mott, N. F. & Davies, E. A. 1979 *Electronic processes in non-crystalline materials* Oxford: Clarendon.

Oelhafen, P., Indlekofer, G. & Günterodt, H.-J. 1988 *Z. Phys. Chem. N.F.* **157**, 483.

Pilgrim, W.-C., Ross, M., Yang, L. H. & Hensel, F. 1997 *Phys. Rev. Lett.* **78**, 3685.

Pilgrim, W.-C., Winter, R., Hensel, F., Morkel, C. & Gläser, W. 1995 *Ber. Bunsenges. Phys. Chem.* **95**, 1133–1136.

Pyykkö, P. 1978 *Adv. Quantum Chem.* **11**, 353.

Rademann, K., Kaiser, B., Even, U. & Hensel, F. 1987 *Phys. Rev. Lett.* **59**, 2319.

Rahman, A. 1974 *Phys. Rev. Lett.* **32**, 52.

Redmer, R. & Warren Jr, W. W. 1993 *Phys. Rev.* B **48**, 14 892.

Redmer, R., Reinholz, H., Röpke, G., Winter, R., Noll, F. & Hensel, F. 1992 *J. Phys. Condens. Matter* **4**, 1659.

Sköld, K., Rowe, J. M., Ostrowski, G. & Randolph, P. D. 1972 *Phys. Rev.* A **6**, 1107.

Shimoji, M. 1977 *Liquid metals*. London: Acadmic.

Tamura, K. & Hosokawa, S. 1994 *J. Phys. Condens. Matter* **6**, A241.

Uchtmann, H. & Hensel, F. 1975 *Phys. Lett.* **53A**, 239.

Uchtmann, H., Brusius, U., Yao, M. & Hensel, F. 1988 *Z. Phys. Chem. N.F.* **156**, 151.

Warren, W. W. & Hensel, F. 1982 *Phys. Rev.* B **26**, 5980.

Warren Jr, W. W., Brennert, G. F. & El-Hannany, U. 1989 *Phys. Rev.* B **39**, 4038.

Weir, S. T., Mitchell, A. C. & Nellis, W. J. 1996 *Phys. Rev. Lett.* **76**, 1860.





PHILOSOPHICAL TRANSACTIONS OF THE ROYAL SOCIETY A MATHEMATICAL, PHYSICAL & ENGINEERING SCIENCES

Wilson, A. H. 1931 *Proc. R. Soc. Lond.* A **133**, 458.
Winter, R., Bodensteiner, T., Gläser, W. & Hensel, F. 1987 *Ber. Bunsenges. Phys. Chem.* **91**, 1327.
Yao, M. 1994 *Z. Phys. Chem.* **184**, 73.
Yao, M. & Hensel, F. 1996 *J. Phys. Condens. Matter* **8**, 9547.
Yonezawa, F. & Ogawa, T. 1982 *Suppl. Prog. Theor. Phys.* **72**, 1.

## *Discussion*

P. P. Edwards (*School of Chemistry, University of Birmingham, UK*). (i) Could I just ask about the Landau-Zeldovitch (1943) idea. My impression is that (as Professor Hensel has indicated) metals should have two critical points, as first proposed by Landau and Zeldovitch, and thus a discontinuous metal–non-metal transition in a pure fluid might in principle take place either in the liquid or in the vapour phase.

(ii) The metal–non-metal transition, if one exists, must imply a fundamental, qualitative change from metallic to other interatomic forces, and therefore corresponding changes in thermodynamic properties must also occur. (I believe that Krumhansl, amongst others, has discussed this.) Does this argument, therefore, always lead one to the picture of a coincident metal–non-metal transition and thermodynamic phase transition?

(iii) I agree completely with Professor Hensel that the question of detecting experimentally, and realizing theoretically, the precise condition for the metal–non-metal transition at such elevated temperatures is still a major challenge. Is the Ioffe–Regel (mean free path) criterion still the 'best' (i.e. the most robust) indicator of the transition in fluid metals at high temperatures?

F. Hensel. (i) In 1943, Landau and Zeldovitch called attention to the possibilities raised by the interplay between the liquid–vapour and metal–non-metal transitions in fluid metals. While pointing out that a rigorous distinction between a metal and a non-metal can only be made at absolute zero, they nevertheless proposed that the metal–non-metal transition should introduce additional lines of first-order transitions in the phase diagram. They suggested three possible phase diagrams which correspond to situations in which the first-order metal–non-metal transition occurs, wholly in the subcritical liquid or vapour phase, or it coincides with the vapour pressure curve and its prolongation into the critical isochore.

(ii) The existence of the metal–non-metal transition indeed implies that throughout the fluid range of a metal the electronic structure changes significantly with density and temperature, and this implies indeed that the nature of interactions between atoms in a fluid metal depends on the thermodynamic state of the system. For example, liquid mercury near its triple point is in equilibrium with a low density, nonmetallic vapour phase. In such a situation there is general agreement that a metal–non-metal transition coincides precisely with the liquid–vapour transition. Both the density and the interparticle interactions change on passing from one phase to the other. It must be emphasized, however, that this general agreement is based on the fact that no one seriously questions the designation of liquid mercury as a metal at its triple point. However, as pointed out by Landau & Zeldovitch, a rigorous distinction between a metal and a non-metal can only be made at absolute zero. At non-zero temperature, thermal excitation of conduction electrons blurs the difference between metals and non-metals. Various approximate criteria exist for defining a boundary between the metallic and non-metallic states but there is no

rigorous definition valid for a fluid at 'high temperatures'. In particular, as far as I know, there is no single framework for a quantitative prediction of properties over the full range from dense metal to dilute non-metal. Theoretical attempts to model the statistical mechanics of the metal–non-metal transition and its interrelation to the liquid–vapour phase transition reach similar conclusions as Landau & Zeldovitch but are still insufficient to prove a clear cut answer to the question from theory. (iii) It was pointed out by Ioffe and Regel that there exists a natural limit of the nearly free electron theory when the electron mean free path becomes comparable to the mean interparticle distance and conventional weak-scattering theory is no longer valid. Electronic transport in this situation involves multiple scattering and is best described as a diffusive movement of electrons from atom to atom. This state is still metallic, but there is a loss of phase coherence in the wave function on a distance scale comparable with the interparticle distance. The physical conditions at which the conductivity of a particular system reaches the value of the Ioffe–Regel limit is often, and rather arbitrarily, cited as the limit of metallic behaviour. This is merely a convenience, however, because one usually has little knowledge of the actual character of the electronic wave functions in this range.

R. McGreevy (*Studsvik Neutron Research Laboratory, Sweden*). What is the lifetime of a dimer in low density Cs above the critical point?

F. Hensel. The interpretation of the neutron scattering results of $S(Q,\omega)$ for low density liquid rubidium approaching the critical point is based on the assumption that the lifetime is larger than one vibrational period, i.e. larger than $1.2 \times 10^{-12}$ s. This is consistent with the explanation of the behaviour of the Korringa ratio in expanded caesium given by Warren *et al.* (1989). They have developed a semiquantitative description of the Korringa ratio behaviour in terms of enhancement of the dynamic, nonuniform susceptibility. From this point of view, the observed increase in the Korringa ratio at low density is seen to reflect a change in the character of electron spin fluctuations from ferromagnetic enhancement in the normal metal to antiferromagnetic enhancement in the expanded metal. The development of antiferromagnetic spin fluctuations in the expanded liquid metal then leads naturally to the formation of spin-paired species such as the alkali dimer $Cs_2$ in the critical region and in the dense vapour with a lifetime greater than $10^{-12}$ s.

C. N. R. Rao (*Indian Institute of Science, Bangalore, India*). (i) Is there no evidence for clusters such as $Cs_{13}$ in the vapour phase, which would be important in Professor Hensel's chemical model?

(ii) How does Professor Hensel reconcile the information on metallicity of clusters (e.g. non-metallic behaviour in clusters of about 100 atoms or less) with his results?

F. Hensel. (i) Measurements of the optical and magnetic properties of alkali metal vapours show that the dominant species in the vapours are the neutral atom and dimer. The dimer concentration increases sharply on approaching the critical point. A crude interpretation of the magnetic susceptibility (Freyland 1979) suggests a dimer concentration of 30% at about half the critical density. There is up to now no experimental evidence for the existence of larger clusters in the vapour.

(ii) In view of the intimate link between the critical density fluctuations and the strong variations of macroscopic properties observed in the course of the metal–non-metal transition, cluster models which consider large and fluctuating clusters seem to be appropriate for the metal–non-metal transition range (see Fisher 1967). The

presence of such clusters naturally raises the question whether such aggregates can be considered as macroscopic entities having the properties of the corresponding bulk. A small cluster of metal atoms differs from the bulk by having a low density of states near the Fermi level and discrete energy levels leading to certain quantum size effects, i.e. the aggregates behave more like normal large molecules with a sparse distribution of filled and empty levels. The energy level splittings between the highest occupied and the lowest unoccupied energy levels may be large compared to the thermal energy $kT$ so that optical, dielectric, magnetic and electrical properties can be very different from those typical of a metal. The answer to the question 'At what size of the cluster does the electronic energy level splitting become so small compared to $kT$ that the cluster may be considered metallic?' depends on the detailed nature of the atoms concerned. For example, it is quite possible that some of the experimentally observed differences in the electronic properties of mercury clusters with respect to other divalent-metal clusters, such as $Mg_n$ and $Be_n$ may have a relativistic origin.

*Additional references*

Fisher, M. E. 1967 *Physics* **3**, 255

Freyland, W. 1979 *Phys. Rev.* B **20**, 5104.

Warren, W. W., Brennet, G. F. & El-Hanany, U. 1989 *Phys. Rev.* B **39**, 4038.





PHILOSOPHICAL TRANSACTIONS OF THE ROYAL SOCIETY A MATHEMATICAL, PHYSICAL & ENGINEERING SCIENCES

PHILOSOPHICAL TRANSACTIONS OF THE ROYAL SOCIETY A MATHEMATICAL, PHYSICAL & ENGINEERING SCIENCES